J Nanostruct Chem (2015) 5:205–212
DOI 10.1007/s40097-015-0151-4

ORIGINAL

Surface passivation by L-arginine and enhanced optical properties of CdS quantum dots co-doped with Nd^{3+}–Li^{+}

S. S. Talwatkar · A. L. Sunatkari · Y. S. Tamgadge · V. G. Pahurkar · G. G. Muley

Received: 17 December 2014 / Accepted: 16 February 2015 / Published online: 4 March 2015

Abstract L-Arginine-passivated Nd^{3+} and Li^{+} co-doped CdS quantum dots (QDs) were synthesized by chemical precipitation method. Ultraviolet–visible absorption spectra of prepared QDs show absorption in the range of 477–450 nm indicating huge blue shift in energy band gap as compared to the bulk CdS due to quantum confinement effect. The optical band gap is found increasing from 2.44 to 2.97 eV as the doping concentration increased from 1 to 5 wt%. Photoluminescence spectra showed that co-doped CdS QDs are highly luminescent and emit multiple intense violet (362, 371, 385, 395 nm) and blue (422, 445, 456 and 465 nm) coloured peaks with increasing intensity with co-dopant concentration. Fourier transform infrared study confirmed the interaction between CdS nanoparticles and L-arginine ligands. The structural and morphological study revealed the formation of orthorhombic crystal structure. The size of CdS QDs, as analysed by X-ray diffraction and high-resolution transmission electron microscopy, is found reducing with co-dopant concentration. The energy dispersive X-ray analysis shows no impurities present except dopants indicating high purity of the prepared samples. Based on the results, we proposed that this material is a new class of luminescent material suitable for optoelectronics devices' application, especially in light emitting devices, electroluminescent devices and display devices.

Keywords CdS quantum dot · Nd^{3+}–Li^{+} co-doping · L-Arginine capping · Blue–violet emission

Introduction

The last two decades have witnessed a tremendous growth and improvisation in investigating and developing semiconductor nanoparticles in the field of basic and applied research. The semiconducting nanoparticles are of great importance due to their unique physical and chemical properties. The structural aspects and optical properties such as photoconductivity and photoluminescence of nanoparticles are substantially different from their bulk counterparts attributed to the quantum confinement effect and large surface to volume ratio of atoms. Group II–IV semiconductor nanoparticles have wide applications in optoelectronics, photonics, solar cell, photo-detector, laser, light emitting diodes, and high-density magnetic information storage [1–7]. Among the chalcogenide materials, CdS is widely investigated due to its intrinsic direct band gap of 2.42 eV at room temperature, which can be exploited in potential device applications involving bio-imaging,

S. S. Talwatkar
Department of Physics, N. G. Aacharya and D. K. Marathe College of Arts, Science and Commerce, Chembur, Mumbai 400071, Maharashtra, India
e-mail: swarna_81@rediffmail.com

A. L. Sunatkari
Department of Physics, Siddharth College of Arts, Science and Commerce, Fort, Mumbai 400001, Maharashtra, India
e-mail: ashok.sunatkari@rediffmail.com

Y. S. Tamgadge
Department of Physics, Shri Shivaji Arts, Commerce and Science College, Akola 444003, Maharashtra, India
e-mail: ystamgadge@gmail.com

V. G. Pahurkar · G. G. Muley (✉)
Department of Physics, Sant Gadge Baba Amravati University, Amravati 444602, Maharashtra, India
e-mail: gajananggm@yahoo.co.in

heterogeneous photo catalysis, nonlinear optics and many more [8–11].

Since Bhargava and co-worker [12] reported significant enhancement in photoluminescence in Mn^{2+} doped ZnS nanoparticles, doping method has been widely used to alter the physical and chemical properties of CdS quantum dots (QDs). Dopant ions interact with host atoms and may bring electronic state within the band gap rendering peculiar properties to the material [13, 14]. CdS QDs with various metal dopants of different concentrations and size controlling capping agents have studied for their tunable band gap, size-dependant optical properties, chemical stability, and easy preparation techniques [15]. The location of dopant in the host material produces changes in properties of CdS QDs. Transition metals such as cobalt, manganese, copper and nickel-doped CdS nanoparticles have widely attracted the scientific attention due to their unique optical properties and their potentiality for various applications [16–20]. In the recent years, researchers have diverted their attention to co-doped CdS QDs with dopant combinations such as Ni^{2+}–Mn^{2+}, Pb^{2+}–Cu^{2+}, Cu^{+}–Cu^{2+}, Co^{2+}–Cu^{2+}, Cu–Al, Mn^{2+}–Eu^{3+}, Cu^{2+}–In^{3+}, Li^{+}–RE^{3+} and Cu^{2+}–RE^{3+} (RE-rare earth) to explore the possibility of enhanced photoluminescence [21–26]. In addition, surface passivation also plays a vital role in the enhancement of optical properties, especially photoluminescence. Numerous reports are available on the influence of surface passivation on improving linear optical properties of CdS QDs [27]. Amino acids are inherently compatible, and one of the common amino acids is L-arginine, which has zwitterionic structure. Hence, functionalization of CdS QDs with L-arginine molecule highly facilitates the interaction of nanoparticles with functional groups and has potential to bring drastic changes in optical properties. Earlier, L-arginine has been demonstrated a good surface-modifying agent in the preparation of ZnO and ZnS nanoparticles [7, 19, 26]. Therefore, we have used L-arginine as capping agent in the synthesis of CdS QDs.

Several methods such as ultraviolet (UV) irradiation, gamma irradiation, microwave irradiation, salvo-thermal method, and thermal decomposition were used for the synthesis of CdS QDs and characterized to explore their important technological applications [28–31]. The easiest and cost effective method is chemical co-precipitation method, can be carried at room temperature, and used extensively to obtain innumerable kinds of functional CdS QDs.

In this paper, we report the synthesis of Nd^{3+}–Li^{+} co-doped CdS QDs by chemical co-precipitation method using L-arginine as surface-modifying agent. More emphasis laid on the possible effect of co-doping on physical and optical properties of CdS QDs. The synthesized QDs were characterized by ultraviolet–visible (UV–vis) spectroscopy, Fourier transform infrared (FT-IR) spectroscopy, photoluminescence (PL), powder X-ray diffraction (XRD), high-resolution transmission electron microscopy (HR-TEM) and energy dispersive X-ray spectroscopy (EDAX).

Materials and methods

Materials

All chemicals, cadmium chloride ($CdCl_2$), sodium sulphide (Na_2S), neodymium oxide (Nd_2O_3), lithium chloride (LiCl), and L-arginine of analytical grade purity purchased from Sigma-Aldrich Germany, are used as received without any further purification. Double distilled water is used in the synthesis process.

Synthesis of CdS QDs

CdS QDs are synthesized using chemical reduction method. 0.5 M stock solutions of cadmium chloride, L-arginine, sodium sulphide, and lithium chloride were prepared separately in double distilled water. 0.5 M solution of neodymium oxide was prepared by dissolving an appropriate amount in hydrochloric acid and diluting it by adding double distilled water. Three round bottom flasks were taken for the preparation of 1, 2 and 5 wt% co-doped CdS QDs. 3 mL solution of 0.5 M cadmium chloride was added into each of the three flasks containing 100 ml double distilled water. Stoichiometric amounts of neodymium oxide and lithium chloride solutions were added into three round bottom flasks under vigorous stirring amounting to 1, 2, and 5 wt% Nd^{3+} and Li^{+} co-doped CdS NPs. The mixtures were stirred for 30 min continuously. 1 mL L-arginine from stock solution was added to these mixtures and stirred for another 1 h. Finally, 3 mL sodium sulphide solution (0.5 M), used as a reducing agent, was added drop by drop to the mixtures under constant stirring which immediately resulted in precipitation of CdS QDs followed by colour change of solution to yellow and stirring continued for 2 h to yield a homogeneous yellow precipitate. The precipitate was centrifuged for 25 min at 3500 rpm. The precipitate washed with methanol followed by double distilled water several times and dried under optical heating at 40 °C temperature for 16 h to remove water and other volatile impurities incorporated during the synthesis process. The product was crushed into powder form and used for further study.

Characterization

UV–vis spectrophotometer (Black-C-SR-50, Stellarnet, USA) was used to record absorption and transmission

spectra in the spectral range 200–800 nm. PL spectra were recorded using FL spectrophotometer (F-7000, Hitachi, Japan) in the range of 200–600 nm using excitation wavelength 254 nm. Average size and shape of QDs were determined by HR-TEM using an instrument (JEM-2100F, JEOL, Japan) and point-to-point resolution of 0.19 nm. Powder XRD spectra were recorded using Rigaku rotating anode (H-3R) diffractometer (MiniFlex II) with irradiation from Kα line of copper ($\lambda = 1.5418$ Å) and angle 2θ ranging from 20° to 80°. FT-IR spectra were obtained with instrument Hyperion microscope with vertex 80 FT-IR system (3000, Bruker, Germany) in the range of 450–7500 cm^{-1}.EDAX analysis has been done with the help of FEG-SEM instrument (JSM 7000F, JEOL, Japan) having resolution 1.0 nm with accelerating voltage 15 kV.

Results and discussion

UV–vis spectroscopy

The UV–vis absorption spectra of Nd^{3+}–Li^{+} co-doped CdS QDs were recorded at room temperature in the wavelength range of 200–800 nm and depicted in Fig. 1. The sharp nature of absorption edge was attributed to the relatively narrow particle size distribution due to quantum confinement effect. This phenomenon reflects more confinement of excitons due to the increased oscillator strength [23]. Highest intensity peak appears for 5 wt% co-doping concentration. The absorption edge of bulk CdS is at 515 nm (2.43 eV); while in our prepared samples the absorption peak position is observed at 477, 463, and 450 nm for 1, 2 and 5 wt% co-dopant concentration, respectively. The band gap estimated from wavelength of absorption is 2.60, 2.70 and 2.72 eV for 1, 2 and 5 wt% co-dopant concentration, respectively. This indicates very large blue shift. The blue shift is caused by the confinement of electrons and holes in extremely small volume of space and formation of smaller sized QDs as co-dopant concentration increases [24]. It is also noticed that as the (Nd^{3+}–Li^{+}) concentration increases from 1 to 5 wt%, the absorption edge shifts to lower wavelength side and intensity increases with increasing (Nd^{3+}–Li^{+}).

The more accurate values of band gap can be obtained using Tauc relation [32, 33] given by $\alpha h\nu = k(h\nu - \Delta E_g)^{1/2}$, where k is constant, α is the absorption coefficient, and ΔE_g is band gap of the material. A plot of $(\alpha h\nu)^2$ against energy ($h\nu$) gives direct band gap of nanoparticles as illustrated in Fig. 2. Linear part of curve is extrapolated to $h\nu$ axis to find band gap. The band gap is found to be 2.44, 2.76 and 2.97 eV for 1, 2 and 5 wt% co-doping concentration of (Nd^{3+} + Li^{+}), respectively, which agrees excellently with the band gap calculated from absorption spectra. Figure 2 shows that the band gap of CdS QDs increases with the increase in doping concentration from 1 to 5 wt%.

The band gap obtained from the above graph is used to calculate the size of the co-doped CdS QDs using Bruce's effective mass approximation (EMA) method [34]. This method gives the energy of nanoparticles in the lowest state 1 s as a function of radius. The total energy of the nanoparticles can be written as $E_{np} = E_{bulk} + E_{coul} + E_{conf}$, where E_{np} is the band gap of nanoparticles, E_{bulk} is band gap of CdS bulk (2.43 eV), E_{confo} is kinetic energy due to electron–hole pair confinement and E_{coul} is coulomb interaction energy of electron–hole. The E_{np} is given by

$$E_{np} = E_{bulk} + \frac{\pi^2\hbar^2}{2R^2}\left(\frac{1}{m_e^*} + \frac{1}{m_h^*}\right) + \frac{-1.8e^2}{4\pi\varepsilon_0\varepsilon_r R} \quad (1)$$

where R is the radius of nanoparticles, $m_h^* = 0.8m_e$ and $m_e^* = 0.19m_e$ are effective masses of electron and hole, respectively. ε_0 is the permittivity of free space and ε_r is

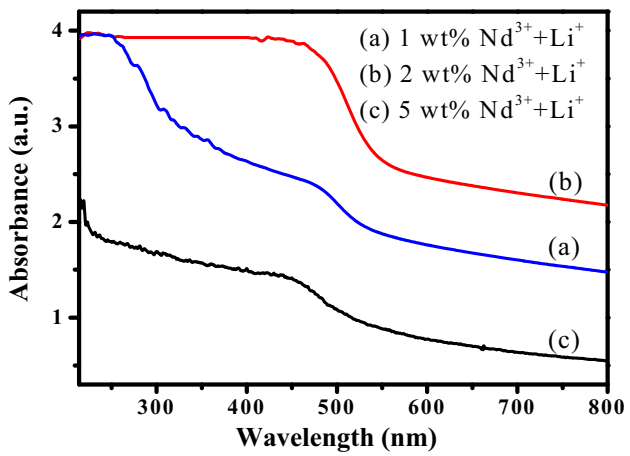

Fig. 1 UV–vis absorption spectra of CdS QDs with *a* 1, *b* 2, and *c* 5 wt% of (Nd^{3+} + Li^{+}) co-doping

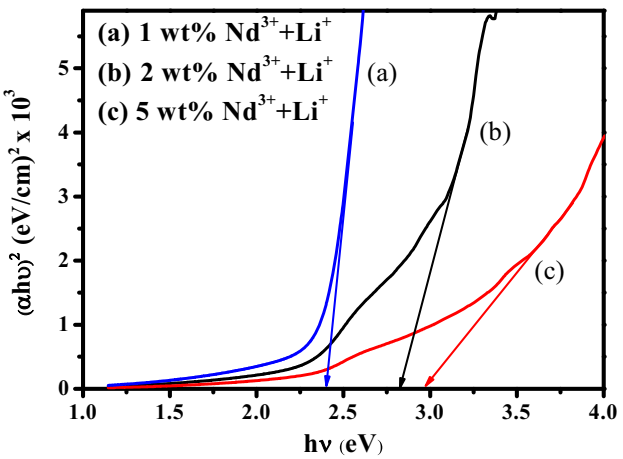

Fig. 2 Graph of $h\upsilon$ vs. $(\alpha h\upsilon)^2$ for *a* 1, *b* 2 and *c* 5 wt% of (Nd^{3+} + Li^{+}) co-doping

dielectric constant ($\varepsilon_r = 5.7$) for CdS. Second term in the equation is related to quantum confinement effect which leads to blue shift. In strong quantum confinement effect, coulomb term is very small and can be neglected [34–37]. In this experiment, since particle size is very small due to strong confinement, we have neglected coulomb term. With the help of Bruce's equation, the sizes of the CdS QDs are estimated at 6.4, 5.4 and 5.0 nm corresponding to 1, 2 and 5 wt% doping concentration of ($Nd^{3+} + Li^{+}$), respectively.

Photoluminescence properties

Figure 3 shows PL spectra of L-arginine-capped Nd^{3+}–Li^{+} co-doped CdS QDs recorded at room temperature in the spectral range of 300–600 nm with excitation wavelength at 254 nm. Luminescence observed in semiconductor nanoparticle is mainly due to the excitonic emission and emissions from trapped state. Excitonic emission is sharp in nature and can be present near absorption edge, if material is pure. However, if material doped with impurities then a broad and intense emission can occur at higher wavelength due to the recombination of charge carriers at the trapped states [38]. The possible sources of presenting luminescence peaks reported by Kharazmi et al. [11] are free excitonic recombination, band-edge transition, transitions from exciton band to neutral acceptor, donor to acceptor conduction band to interstitial sulphur (green emission), interstitial cadmium to valence band (yellow emission), sulphur vacancy to valence band (red emission), and cadmium vacancy to the valence band.

The PL spectra reveal that the sharp emission peaks with highest intensity are located at 445 nm for pure CdS QDs whereas for 1, 2 and 5 wt% of ($Nd^{3+} + Li^{+}$) co-doping, emission peak is shifted to lower wavelength side (blue shift) and appears at 439,438 and 431 nm, respectively, due to band-edge emission. In addition, for 1 wt% co-doping, a weak emission peak at 422 nm is observed, whereas for 2 wt% co-dopant concentration, two weak peaks at 371 and 395 nm have been found along with shoulder at 465 nm. Similar emission peaks are also located in the spectra for 5 wt% co-dopant concentration viz. two weak peaks at 362, 385 and shoulder at 456 nm. Nd^{3+} and Li^{+} ions may either exist in the CdS host lattice or attach to the outside surface with capping agent. These multiple peaks may be due to the existence of different type of Nd^{3+} and Li^{+} centres in the CdS QDs and capping agent band structure [39]. The broad emission peaks at 371, 395, 430 and 456 nm are mainly because of surface trap-state emission. The trap-state emission is due to defects on the interface between QDs and capping agent [10]. The shoulders at ~469 and 456 nm are attributed to the excitonic emission of CdS QDs. Further it is noticed from PL spectra that the intensity of emission peak increases as the doping concentration increased from 1 to 5 wt%. Nazerdeylami et al. [40] have reported similar intensity-trend. Moreover, PLE results show that smaller QDs have higher intensity of band-edge emission compared to trap-state emission. The intensity of band-edge emission and trap-state emission becomes comparable for the 5 wt% co-doping concentration. The probable reason for this may be due to the fact that the smaller QDs have large number of atoms on the surface leading to more amorphous structure and, hence, intense trap-state photoluminescence. Finally, PL spectra of our sample indicate that Nd^{3+} and Li^{+} ions are successfully entrenched into the CdS lattice producing enhanced luminescence properties. To obtain better understanding of role of Nd^{3+} and Li^{+} ions in enhancement of photoluminescence intensity, high-resolution PL and site-selective PL measurements are required [40, 41].

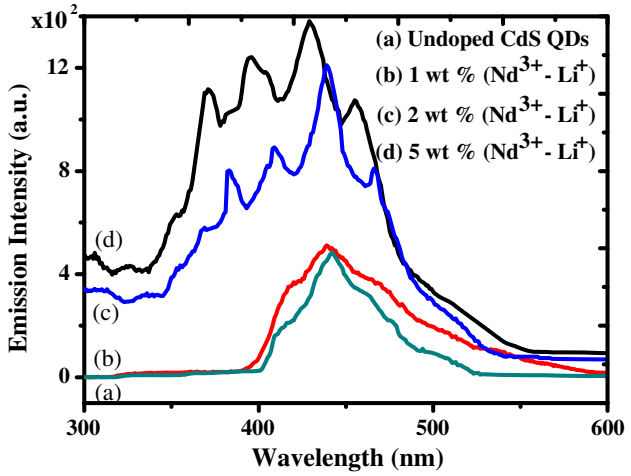

Fig. 3 Emission spectra of *a* undoped and *b* 1, *c* 2, *d* 5 wt% of ($Nd^{3+} - Li^{+}$) doped CdS QDs (excitation at $\lambda_{ex.} = 254$ nm)

FT-IR studies

Figure 4 depicts FT-IR spectra of L-arginine, pure CdS and L-arginine-passivated CdS QDs. In the FT-IR spectrum of L-arginine (Fig. 4a), peaks in the higher energy regime 3469–2776 cm^{-1} are attributed to the C–H, O–H, $–NH_3^{+}$ and N–H stretching's. C=O stretching presents an absorption band at ~1517 cm^{-1}. The absorption centred at ~1465 cm^{-1} is due to C–H and N–H deformations, while the peak at 1372 is assigned to C–H deformation, C=O stretching, and N–H deformation. C–H deformation also casts its absorptions at 1224, 993, 909, 783 and 553 cm^{-1}. In addition to the C–H deformation, the absorption at 1224 cm^{-1} may be attributed to the C=O and C–O stretching, and O–H deformation. Strong absorption at

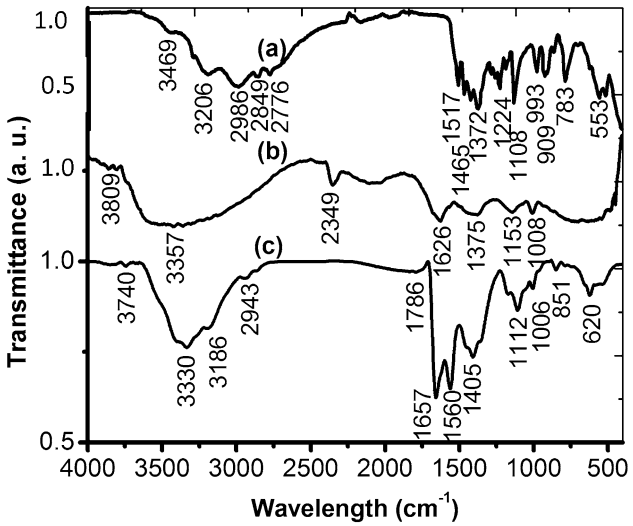

Fig. 4 FT-IR spectrum of *a* L-arginine, *b* pure CdS and *c* L-arginine-passivated CdS QDs

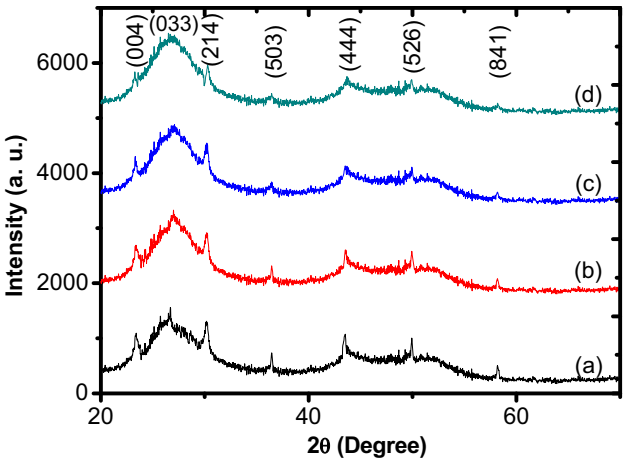

Fig. 5 Powder XRD spectra of *a* un-doped CdS QDs, and co-doped with *b* 1, *c* 2, and *d* 5 wt% of (Nd^{3+} − Li^{+})

1108 cm^{-1} is assigned to C–O stretching. The spectrum of pure CdS (Fig. 4b) exhibiting an absorption peak at ~1008 cm^{-1} may be assigned to the stretching vibrations of the CdS. Absorptions at ~1153 and 1375 cm^{-1} are due to the bonding between S and O of absorbed H_2O and ethanol and absorption at ~1626 cm^{-1} is assigned to the bending vibrations of H_2O. The peaks around 2349, 3357 and 3809 cm^{-1} are due to the O–H stretching. L-arginine exhibits zwitterionic structure which may be responsible for effective passivation of CdS nanoparticles. The displacement of peak 1108 cm^{-1}, assigned to the C–O stretching, to the 1112 cm^{-1} in L-arginine-passivated CdS QDs (Fig. 4c) confirms the involvement of –COOH group of L-arginine in passivation mechanism. The broad absorption in higher energy regime instead of sharp peaks prompts the strong modifications around $–NH_3^+$ and $–COO^-$ groups of L-arginine which are responsible to minimize the field of CdS and prevent from allogomeartion and crystallization.

The displacement and variation in absorption strength of other peaks such as 1517, 1372 and 993 cm^{-1} of L-arginine in L-arginine-passivated CdS advocate effective passivation of CdS QDs and interaction between CdS and L-arginine [42–44].

Structural and morphological study

Figure 5 shows the powder XRD pattern of as-prepared 5 wt% (Nd^{3+} + Li^{+}) co-doped CdS QDs. The XRD pattern divulges the crystalline phase and crystalline size of CdS QDs. The diffraction peaks were observed at $2\theta = 24.44°$, 25.30°, 26.50°, 28.55°, 36.41°, 43.79°, 50.95°, 51.81°, 58.20°, 60.92° and 66.90° corresponding to crystal planes (0 0 4), (0 4 0), (0 3 3), (2 1 4), (5 0 3), (4 4 4), (5 2 6), (0 2 8), (8 4 1), (6 6 4), and (2 2 1), respectively. It is noticed from the spectra that the peaks became broad as the doping concentration increased from 1 to 5 wt%. The d-spacing values and relative intensity of peaks match well with JCPDS data (PDF No. 047-1179) of CdS for orthorhombic structure with crystal lattice parameters $a = 14.31$, $b = 14.07$ and $c = 14.56$ Å. Broadening of the peaks is due to the formation of small sized QDs. In addition, no diffraction peaks of impurities (including dopants) are detected. This indicates that the samples are pure in nature and also suggests that Nd^{3+} and Li^{+} ions have entered into the CdS lattice as a substituent [45]. The large full width at half maxima (FWHM) and decrease in intensity of the peaks with increasing co-dopant concentration suggest the effect of Nd^{3+} and Li^{+} doping on CdS crystallinity.

The crystalline size of CdS QDs has been calculated using Debye–Scherrer equation $2R = 0.9\lambda/\beta\cos\theta$ [46], where $2R$ is the diameter of QDs, β is FWHM of XRD peaks in radian, θ is diffraction angle and λ is wavelength of X-ray (1.54059 Å). The FWHM of peaks (0 4 4), (2 1 4), (5 0 3), (4 4 4) and (8 4 1) are used to estimate the sizes of CdS QDs. The average sizes are found to be 6.8, 5.6, 4.5 and 3.6 nm for undoped, 1, 2, and 5 wt% co-doped CdS QDs, respectively, which indicate that as the co-doping concentration increased from 1 to 5 wt%, the size reduced from 6.8 to 3.6 nm. The comparative chart of sizes of CdS QDs is given in Table 1.

We have calculated the d-spacing from selected area electron diffraction (SAED) pattern and assigned the d [hkl] planes in the pattern as shown in Fig. 6b. We found that d [hkl] planes from SAED pattern fairly agree with the d [hkl] planes given in the literature (PDF No. 047-1179). Figure 6a shows HR-TEM image of CdS QDs along with SAED pattern in Fig. 6b. The low magnified TEM image is

Table 1 Band gap and size of as-prepared CdS QDs

Nd^{3+} and Li^{+} concentration (wt%)	Band gap (eV)	Size estimated from (nm)		
		EMA method	Powder XRD	HR-TEM
1	2.44	6.4	5.6	5.5
2	2.76	5.4	4.5	4.0
5	2.97	5.0	3.6	3.0

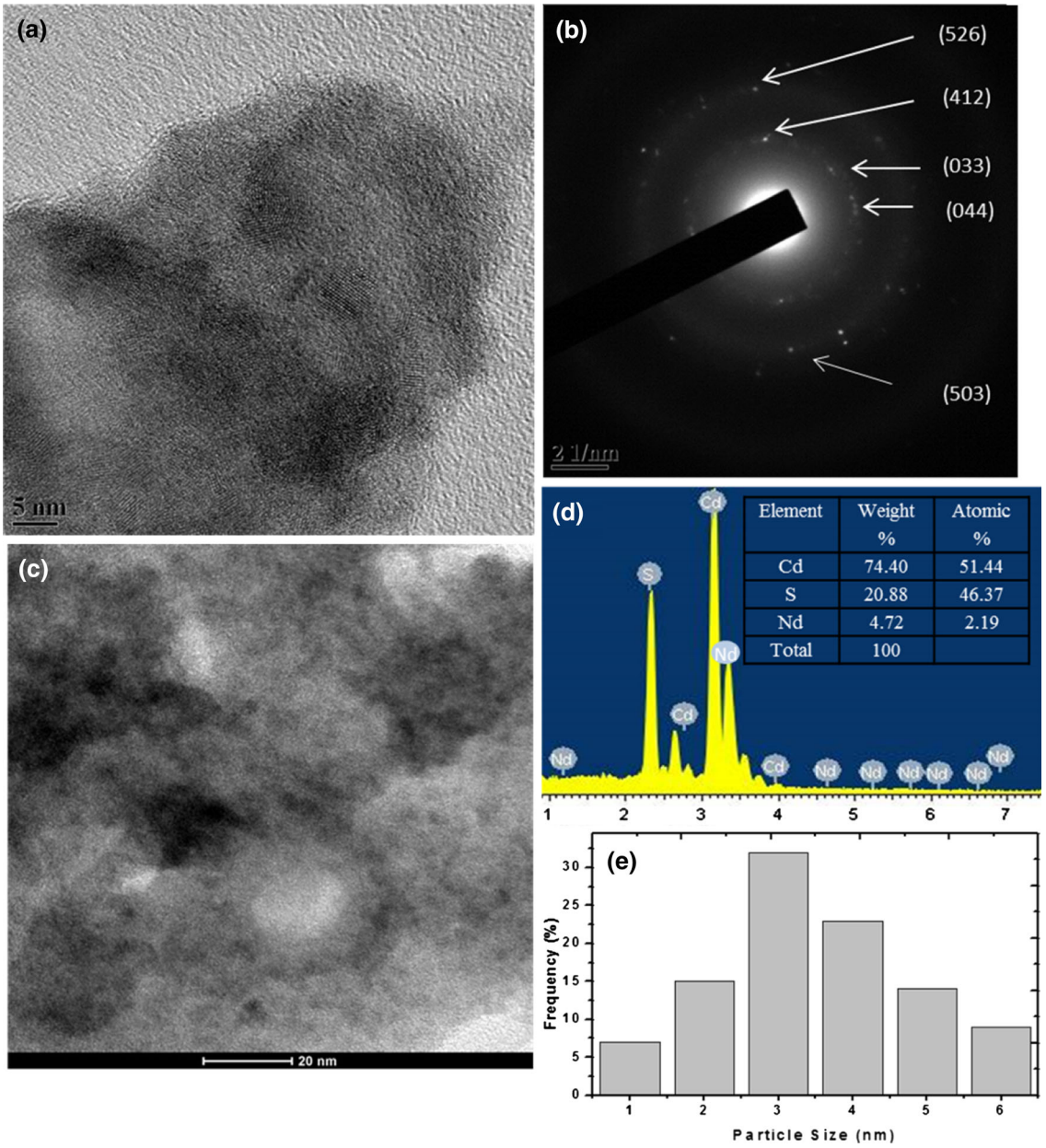

Fig. 6 **a** HR-TEM image, **b** SAED pattern, **c** TEM image, **d** EDAX pattern of 5 wt% (Nd^{3+} + Li^{+}) co-doped CdS QDs (*in inset* atomic and weight percentages are shown) and **e** histogram of particle size distribution

shown in Fig. 6c. The histogram of particle size distribution is shown in Fig. 6e. The sizes of QDs are found in the range of 1.5–7 nm with average size 3.0 nm for 5 wt% co-dopant concentration. The chemical compositions of as-prepared CdS QDs capped with L-arginine confirmed from the energy dispersive X-ray analysis (EDAX) pattern are

represented in Fig. 6d. EDAX spectrum indicates the presence of Cd, S, and Nd elements. Lithium being a lighter element is undetected by the instrument. NMR spectroscopy can be used to detect the presence of Li into CdS QDs, site symmetry as well as its diffusion behaviour, but cannot give information about the quantity. Inductively coupled plasma-atomic emission spectroscopy can be used to find exact quantity of compositional elements, including lithium, present in the samples. The atomic percentages and weight percentage of Cd, S and Nd have found close to the target values, shown in the inset of Fig. 6d.

The sizes of CdS QDs calculated from XRD peaks and HR-TEM match well with the sizes calculated also from Bruce equation (EMA method) too. Table 1 shows comparison of average size of CdS QDs calculated by various methods.

From Table 1, we conclude that the size of CdS QDs is reduced and the band gap increased with the increase in co-doping concentration.

Conclusions

In summary, Nd^{3+} and Li^{+} co-doping effectively alter the structural, morphological and optical properties of nano materials in a way that the increase in the dopant concentration leads to the increase in band gap and decrease in the particle size. Smaller sized and doped QDs are the most preferable material for optics-based applications such as optoelectronics, photonics, solar cells, photo-detectors, lasers and light emitting diodes. Residing on this theory, we have attempted the synthesis of L-arginine passivated CdS QDs co-doped with Nd^{3+} and Li^{+} successfully by following the kinetics of chemical co-precipitation method. L-Arginine was functioned as an excellent stabilizing agent. The structural and morphological study of co-doped CdS QDs revealed the formation of orthorhombic crystal structure. The sizes of CdS QDs reduce with co-dopant concentration. UV–vis spectroscopy illustrated the absorption edge located at wavelengths 477, 463 and 450 nm for 1, 2, and 5 wt% co-doping concentration of ($Nd^{3+} + Li^{+}$), respectively, showing huge blue shift compared to their bulk counterpart due to quantum confinement effect. Band gap of CdS QDs is increased from 2.44 to 2.97 eV. The increase in band gap with the concentration of dopant indicates the effect of co-doping in CdS QDs. PL spectra showed the band-edge emission and trapped-state emission with multiple violet and blue photoluminescent centres whose intensity increases with doping concentration. At 5 wt% doping concentration, the intensity of band-edge emission and trap-state emission became almost equal. EDAX spectra indicated the presence of no other impurities except Cd, S and Nd elements in CdS QDs. These results strongly suggest that our sample possesses a high potential in optoelectronics device applications.

Acknowledgments Authors are thankful to the Director, SAIF, IIT-Bombay for providing FTIR, TEM and EDAX facility and the Chairman, DST-FIST, SGB Amravati University for providing XRD and PL facility. The authors also express special thanks to Dr. S. D. Pawar for timely providing FT-IR spectra of parent sample.

References

1. Chen, W., Ghule, A., Chang, J., Chen, B., Liu, J., Tzing, S.: Synthesis, characterization, photo and physicochemical properties of 11-mercaptoundecanoic acid and tetraaniline capped CdS quantum dots. Mater. Chem. Phys. (2010). doi:10.1016/j.matchemphys.2010.05.049
2. Mane, R., Lokhande, C.: Chemical deposition method for metal chalcogenide thin films. Mater. Chem. Phys. (2000). doi:10.1016/S0254-0584(00)00217-0
3. Lee, W., Mane, R., Min, S., Yoon, T., Han, S., Lee, S.: Nanocrystalline CdS-water-soluble conjugated-polymers: high performance photoelectrochemical cells. Appl. Phys. Lett. (2007). doi:10.1063/1.2752021
4. Dong, W., Zhu, C.: Optical properties of surface-modified CdO nanoparticles. Opt. Mater. (2003). doi:10.1016/S0925-3467(02)00269-0
5. Judd, B.: Optical absorption intensities of rare-earth ions. Phys. Rev. (1962). doi:10.1103/PhysRev.127.750
6. Kamat, P.: Meeting the clean energy demand: nanostructure architectures for solar energy conversion. J. Phys. Chem. C (2007). doi:10.1021/jp066952u
7. Talwatkar, S., Tamgadge, Y., Sunatkari, A., Gambhire, A., Muley, G.: Amino acids (L-arginine and L-alanine) passivated CdS nanoparticles: synthesis of spherical hierarchical structure and nonlinear optical properties. Solid State Sci. (2014). doi:10.1016/j.solidstatesciences.2014.09.014
8. Saikia, D., Saikia, P., Gogoi, P., Das, M., Sengupta, P., Shelke, M.: Synthesis and characterization of CdS/PVA nanocomposite thin films from a complexing agent free system. Mater. Chem. Phys. (2011). doi:10.1016/j.matchemphys.2011.09.011
9. Senthil, K., Mangalraj, D., Narayandass, S.: Structural and optical properties of CdS thin films. Appl. Surf. Sci. (2001). doi:10.1016/S0169-4332(00)00732-7
10. Yordanov, G., Adachi, E., Dushkin, C.: Characterization of CdS nanoparticles during their growth in paraffin hot-matrix. Mater. Charact. (2007). doi:10.1016/j.matchar.2006.05.010
11. Kharazmi, A., Saion, E., Faraji, N., Soltani, N., Dehzangi, A.: Optical properties of CdS/PVA nanocomposite films synthesized using the gamma-irradiation-induced method. Chin. Phys. Lett. (2013). doi:10.1088/0256-307X/30/5/057803
12. Bhargava, R., Gallagher, D.: Optical properties of manganese-doped nanocrystals of ZnS. Phys. Rev. Lett. (1994). doi:10.1103/PhysRevLett.72.416
13. Kalandaragh, Y., Muradov, M., Mamedov, R., Behboudnia, M., Khodayari, A.: J. Optoelectron. Adv. Mater.Rapid Commun. **2**, 42–45 (2008)
14. SaraswathiAmma, B., Manzoor, K., Ramakrishna, K., Pattabi, M.: Synthesis and optical properties of CdS/ZnS core–shell

nanoparticles. Mater. Chem. Phys. (2008). doi:10.1016/j.matchemphys.2008.06.043
15. Dabbousi, B., Rodriguez-Viejo, J., Mikulec, F., Heine, J., Mattoussi, H., Ober, R., Jensen, K., Bawendi, M.: (CdSe) ZnS core–shell quantum dots: synthesis and characterization of a size series of highly luminescent nanocrystallites. J. Phys. Chem. B (1997). doi:10.1021/jp971091y
16. Chandramohan, S., Kanjilal, A., Sarangi, S., Majumder, S., Sathyamoorthy, R., Som, T.: Implantation-assisted co-doped CdS thin films: structural, optical, and vibrational properties. J. Appl. Phys. (2009). doi:10.1063/1.3224867
17. Rathore, K., Patidar, D., Saxena, N., Sharma, K.: Effect of Cu doping on the structural, optical and electrical properties of Cds nanoparticles. J. Ovonic Res. **5**(6), 175–185 (2009)
18. Salimian, S., Farjami Shayesteh, S.: Luminescence properties of manganese doped CdS nanoparticles under various synthesis conditions. Acta Phys. Pol. A **118**, 633–636 (2010)
19. Tamgadge, Y., Sunatkati, A., Talwatkar, S., Pahurkar, V., Muley, G.: Linear and nonlinear optical properties of nanostructured $Zn_{(1-x)}Sr_xO$–PVA composite thin films. Opt. Mater. (2014). doi:10.1016/j.optmat.2014.04.036
20. Jaiswal, J., Mattoussi, H., Mauro, J., Simon, S.: Long-term multiple color imaging of live cells using quantum dot bioconjugates. Nat. Biotechnol. (2003). doi:10.1038/nbt767
21. Colvin, V., Schlamp, M., Alivisatos, A.: Light-emitting diodes made from cadmium selenide nanocrystals and a semiconducting polymer. Nature (1994). doi:10.1038/370354a0
22. Yang, Y., Chen, O., Angerhofer, A., Cao, Y.: Radial-position-controlled doping in CdS/ZnS core/shell nanocrystals. J. Am. Chem. Soc. (2006). doi:10.1021/ja064818h
23. Kaur, K., Singh Lotey, G., Verma, N.: Structural, optical and magnetic properties of cobalt-doped CdS dilute magnetic semiconducting nanorods. Mater. Chem. Phys. (2013). doi:10.1016/j.matchemphys.2013.08.005
24. Murray, C., Norris, D., Bawendi, M.: Synthesis and characterization of nearly monodisperse CdE (E = sulfur, selenium, tellurium) semiconductor nanocrystallites. J. Am. Chem. Soc. (1993). doi:10.1021/ja00072a025
25. Hu, H., Zhang, W.: Synthesis and properties of transition metals and rare-earth metals doped ZnS nanoparticles. Opt. Mater. (2006). doi:10.1016/j.optmat.2005.03.015
26. Talwatkar, S., Sunatkari, A., Tamgadge, Y., Pahurkar, V., Muley, G.: Influence of Li^+ and Nd^{3+} co-doping on structural and optical properties of L-arginine-passivated ZnS nanoparticles. Appl. Phys. A (2014). doi:10.1007/s00339-014-8777-5
27. Lu, S., Lee, B., Wang, Z., Tong, W., Wagner, B., Park, W., Summers, C.: Synthesis and photoluminescence enhancement of Mn^{2+}-doped ZnS nanocrystals. J. Lumin. (2001). doi:10.1016/S0022-2313(00)00238-6
28. Vossmeyer, T., Katsikas, L., Giersig, M., Popovik, I., Diesner, K., Chemseddine, A., Eychmüller, A., Weller, H.: CdS nanoclusters: synthesis, characterization, size dependent oscillator strength, temperature shift of the excitonic transition energy, and reversible absorbance shift. J. Phys. Chem. (1994). doi:10.1021/j100082a044
29. Khanna, P., Kulkarni, M., Singh, N., Lonkar, S., Subbarao, V., Kasi Viswanath, A.: Synthesis of HCl doped polyaniline–CdS nanocomposite by use of organometallic cadmium precursor. Mater. Chem. Phys. (2006). doi:10.1016/j.matchemphys.2005.05.041
30. Bhargava, R., Gallagher, D., Hong, X., Nurmikko, A.: Phys. Rev. Lett. (1994). doi:10.1103/PhysRevLett.72.416
31. Bhargava, R.: Doped nanocrystalline materials—physics and applications. J. Lumin. (1996). doi:10.1016/0022-2313(96)00046-4
32. Tauc, J.: Optical properties of amorphous semiconductors. In: Amorphous and Liquid Semiconductors, pp. 159–220. Springer, US (1974). doi:10.1007/978-1-4615-8705-7_4
33. Rao, S., Kumar, R., Reddy, R., SubbaRao, T.: Preparation and characterization of CdS nanoparticles by chemical co-precipitation technique. Chalcogenide Lett. **8**, 177–185 (2011)
34. Brus, L.: Electron–electron and electron-hole interactions in small semiconductor crystallites: the size dependence of the lowest excited electronic state. J. Chem. Phys. (1984). doi:10.1063/1.447218
35. Brus, L.: Luminescence of direct and indirect gap quantum semiconductor crystallites. MRS Proc. (1992). doi:10.1557/PROC-272-215
36. Brus, L., Szajowski, P., Wilson, W., Harris, T., Schuppler, S., Citrin, P.: Electronic spectroscopy and photophysics of Si nanocrystals: relationship to bulk c-Si and porous Si. J. Am. Chem. Soc. (1995). doi:10.1021/ja00115a025
37. Bhattacharjee, B., Bera, S., Ganguli, D., Chaudhuri, S., Pal, A.: Studies on CdS nanoparticles dispersed in silica matrix prepared by sol–gel technique. Eur. Phys. J. B (2003). doi:10.1140/epjb/e2003-00001-3
38. Manifacier, J., Gasiot, J., Fillard, J.: A simple method for the determination of the optical constants *n*, *k* and the thickness of a weakly absorbing thin film. J. Phys. E (1976). doi:10.1088/0022-3735/9/11/032
39. Suhail, A., Khalifa, M., Saeed, N., Ibrahim, O.: White light generation from CdS nanoparticles illuminated by UV-LED. Eur. Phys. J. Appl. Phys. (2010). doi:10.1051/epjap/2010005
40. Nazerdeylami, S., Saievar-Iranizad, E., Dehghani, Z., Molaei, M.: Synthesis and photoluminescent and nonlinear optical properties of manganese doped ZnS nanoparticles. Phys. B (2011). doi:10.1016/j.physb.2010.10.033
41. Gajbhiye, N., Ningthoujam, R., Ahmed, A., Panda, D., Umare, S., Sharma, S.: Pramana. J. Phys. (2008). doi:10.1007/s12043-008-0050-z
42. Socrates, G.: Infrared and Raman Characteristic Group Frequencies: Tables and Charts, 3rd edn. Wiley, UK (2004)
43. Zhang, J.: Optical Properties and Spectroscopy of Nanomaterials. World Scientific Publishing co. pte. Ltd., Singapore (2007)
44. Muley, G., Rode, M., Pawar, B.: FT-IR, thermal and NLO studies on amino acid (L-arginine and L-alanine) doped KDP crystals. Acta Phys. Pol. A **116**, 1033–1038 (2009)
45. Amaranatha Reddy, D., Divya, A., Murali, G., Vijayalakshmi, R., Reddy, B.: Synthesis and optical properties of Cr doped ZnS nanoparticles capped by 2-mercaptoethanol. Phys. B (2011). doi:10.1016/j.physb.2011.02.062
46. Maurya, A., Chauhan, P.: Structural and optical characterization of CdS/TiO_2 nanocomposite. Mater. Charact. (2011). doi:10.1016/j.matchar.2011.01.014